ISSN 1063-7710, Acoustical Physics, 2017, Vol. 63, No. 5, pp. 531–541. © Pleiades Publishing, Ltd., 2017.
Original Russian Text © P.B. Rosnitskiy, L.R. Gavrilov, P.V. Yuldashev, O.A. Sapozhnikov, V.A. Khokhlova, 2017, published in Akusticheskii Zhurnal, 2017, Vol. 63, No. 5, pp. 489–500.

PHYSICAL ACOUSTICS

On the Possibility of Using Multi-Element Phased Arrays for Shock-Wave Action on Deep Brain Structures

P. B. Rosnitskiy[a], *, L. R. Gavrilov[b], **, P. V. Yuldashev[a], O. A. Sapozhnikov[a], and V. A. Khokhlova[a]

[a] *Moscow State University, Moscow, 119991 Russia*

[b] *Andreyev Acoustics Institute, ul. Shvernika 4, Moscow, 117036 Russia*

**e-mail: pavrosni@yandex.ru*

***e-mail: gavrilov@akin.ru*

Received October 21, 2016

Abstract—A noninvasive ultrasound surgery method that relies on using multi-element focused phased arrays is being successfully used to destroy tumors and perform neurosurgical operations in deep structures of the human brain. However, several drawbacks that limit the possibilities of the existing systems in their clinical use have been revealed: a large size of the hemispherical array, impossibility of its mechanical movement relative to the patient's head, limited volume of dynamic focusing around the center of curvature of the array, and side effect of overheating skull. Here we evaluate the possibility of using arrays of smaller size and aperture angles to achieve shock-wave formation at the focus for thermal and mechanical ablation (histotripsy) of brain tissue taking into account current intensity limitations at the array elements. The proposed approach has potential advantages to mitigate the existing limitations and expand the possibilities of transcranial ultrasound surgery.

Keywords: medical acoustics, high-intensity focused ultrasound, HIFU, shock front, ultrasonic surgery, multi-element therapeutic arrays, KZK equation

DOI: 10.1134/S1063771017050104

INTRODUCTION

Recent years have seen the substantial development of noninvasive (without surgical intervention) methods for irradiating deep brain structures through an intact skull using high-intensity focused ultrasound (HIFU) [1]. In transcranial HIFU surgery, an ultrasonic beam is focused through skull bones to targeted brain regions and, depending on the dose, it introduces their local heating and subsequent thermal destruction [1–5]. This method is successfully used clinically to conduct neurosurgical operations for treating essential tremor [2], intracerebral tumors [3], trigeminal neuralgia [4], and chronic neuropathic pain [5].

It is known that the skull bone is an extremely difficult medium for ultrasound transmission. The thickness and ultrasound attenuation in different skull regions are very inhomogeneous, and sound velocity greatly differs from that in water and soft tissues. Since the mid-20th century, the problem of ultrasound focusing through the skull has been studied by several research teams taking into account possible aberrations due to variations in its thickness and acoustic parameters [6, 7]. A solution to this problem became possible with the development of multi-element phased arrays that have individual control of the signal phase and amplitude at each of the array elements to correct for aberrations, as well as the development of noninvasive magnetic-resonance imaging (MRI) methods to monitor the treatment and ultrasound-induced biological effects [1, 8].

Modern transcranial HIFU surgeries are performed using arrays of the ExAblate clinical system developed by InSightec Ltd. (Israel). The arrays contain 1024 elements accommodated on the surface of a hemisphere of 30 cm diameter fitted around the head of a patient [8]. HIFU irradiation on certain brain regions is performed through an intact skull under MR-imaging the temperature distributions and thus the thermal effect of ultrasound within the irradiated region. The operating frequency range in the most of clinically used systems is 650–720 kHz, while the acoustic power used in clinical applications is under 800 W. It has been shown that for this power, nonlinear acoustic effects can be almost completely neglected and conditions for harmonic wave irradiation are realized at the focus [9].

Despite the undoubted advantages of this clinical system with a large (30 cm in diameter) hemispherical array, certain limitations in its use have been revealed, mainly determined by the danger of overheating and damaging skull bones [8, 10]. For example, such transducer design does not allow the mechanical displacement of the array focus. The array is located around the head of the patient so that its center of curvature is located at the center of the skull, and the directions of rays that connect the array elements and the focus are close to be perpendicular to the skull surface. Otherwise, for oblique incidence, the coefficient of ultrasound transmission through the skull bones and the focal intensity decrease abruptly. Electronic steering of the focus by changing phases at the array elements results, for this system geometry and clinically used frequency of 650 kHz, in satisfactory focusing quality only in a relative proximity to the geometric center of the array. Approximate calculations show that in the case of focusing without aberrations, the region of the electronic focus steering with a boundary determined by a 3 dB intensity drop relative to the maximum intensity, has a radius of 2.1 cm [11]. Increasing the array power to compensate for this loss of intensity at the focus during its electronic steering can result in undesirable overheating of bones. The above factors limit practical application of the existing arrays due to their ability to irradiate only small volumes of the brain in the central part of the head with a radius of approximately 2.5 cm.

To overcome these constraints, it is promising to develop protocols for nonlinear pulsed-periodic irradiation, in which high-amplitude shock fronts are developed in the ultrasound pressure waveform at the focus. The use of such regimes extends the capabilities of HIFU, making it possible to increase the speed and locality of thermal effects [12] and to mechanically ablate tissue [13–15]. A recently proposed method termed boiling histotripsy utilizes irradiation with millisecond-long shock-wave pulses with low duty cycle (<1%) and shock-front amplitudes at the focus of 60–120 MPa [15]. It was shown that such irradiation can induce mechanical destruction of tissue into subcellular fragments in the focal region of the ultrasound beam practically without thermal effects or side effects related to overheating tissues in the near field of the transducer. By changing the pulse duration and repetition rate, it is also possible to accelerate thermal ablation of the targeted tissue and to attain combined mechanical and thermal destruction of tissue without damaging surrounding tissues [15]. First successful results have already been obtained using the boiling histotripsy method for mechanical destruction of brain tissue *in vivo* (open brain of piglets) [16]. A Sonalleve V1 3.0T MR-HIFU array (Philips Healthcare, Cleveland, OH) with an aperture of 12.8 cm and a focal length of 12 cm, i.e., with an aperture angle of approximately 60°, was used. Note that the degree of focusing of ultrasound transducers is often characterized by their F-number, $F_{\#} = F/D$, which is equal to the ratio of the transducer focal length F to its diameter D. For transducers with aperture angle of 60°, the value of F-number is $F_{\#} = 1$ (Fig. 1a, the dotted curve, where α is the half-aperture angle). A typical shock-front amplitude at the focus of the Sonalleve system was 80 MPa; in this case, the value of the peak negative pressure was 14 MPa [17].

Unfortunately, it is technically almost impossible to achieve shock-wave mediated effects in tissue when operating with hemispherical array of the ExAblate system. Figure 1a shows the distributions of acoustic pressure magnitude calculated in the linear-focusing approximation using the Rayleigh integral [18] on the axis of a hemispherical transducer with geometric parameters analogous to those for the ExAblate system ($F_{\#} = 0.5$, Fig. 1a, solid curve) and on the axis of a transducer with smaller aperture angle of 60° ($F = D =$ 20 cm, $F_{\#} = 1$) (Fig. 1a, dotted curve). The results illustrate that the length of the main focal lobe for the hemispherical array is much shorter compared to the length of the focal lobe produced by the transducer in the form of a less focused spherical segment. Accumulation of nonlinear propagation effects mainly occurs in the high-amplitude focal region of the beam. Therefore, for a very short focal region of the ExAblate-type array, shock fronts will form at extremely high focal pressure levels [19]. In order to provide such high focal pressures, extremely high transducer power would be required which is rather dangerous for clinical use due to the possibility of damaging the skull bones and induction of cavitation in tissue in the prefocal area of the beam.

Current treatment envelope of the ExAblate hemispherical array systems is therefore limited to the linear focusing of harmonic waves (Fig. 1b) and heat-induced tissue ablation close to the center of the array curvature. On the contrary, with the use of an array in the shape of a spherical segment with an aperture angle of 60°, it is possible to generate a nonlinear waveform (Fig. 1c) with the shock amplitude of 80 MPa, which is applicable for both mechanical and thermal action on tissue at the focus without damaging overlaying tissues [13, 15, 16]. However, it is still unclear whether this approach is feasible taking into account the effects of aberrations, ultrasound reflection, and absorption losses when focusing through the skull bones and brain tissues, as well as existing technical limitations on the initial intensity at the array elements.

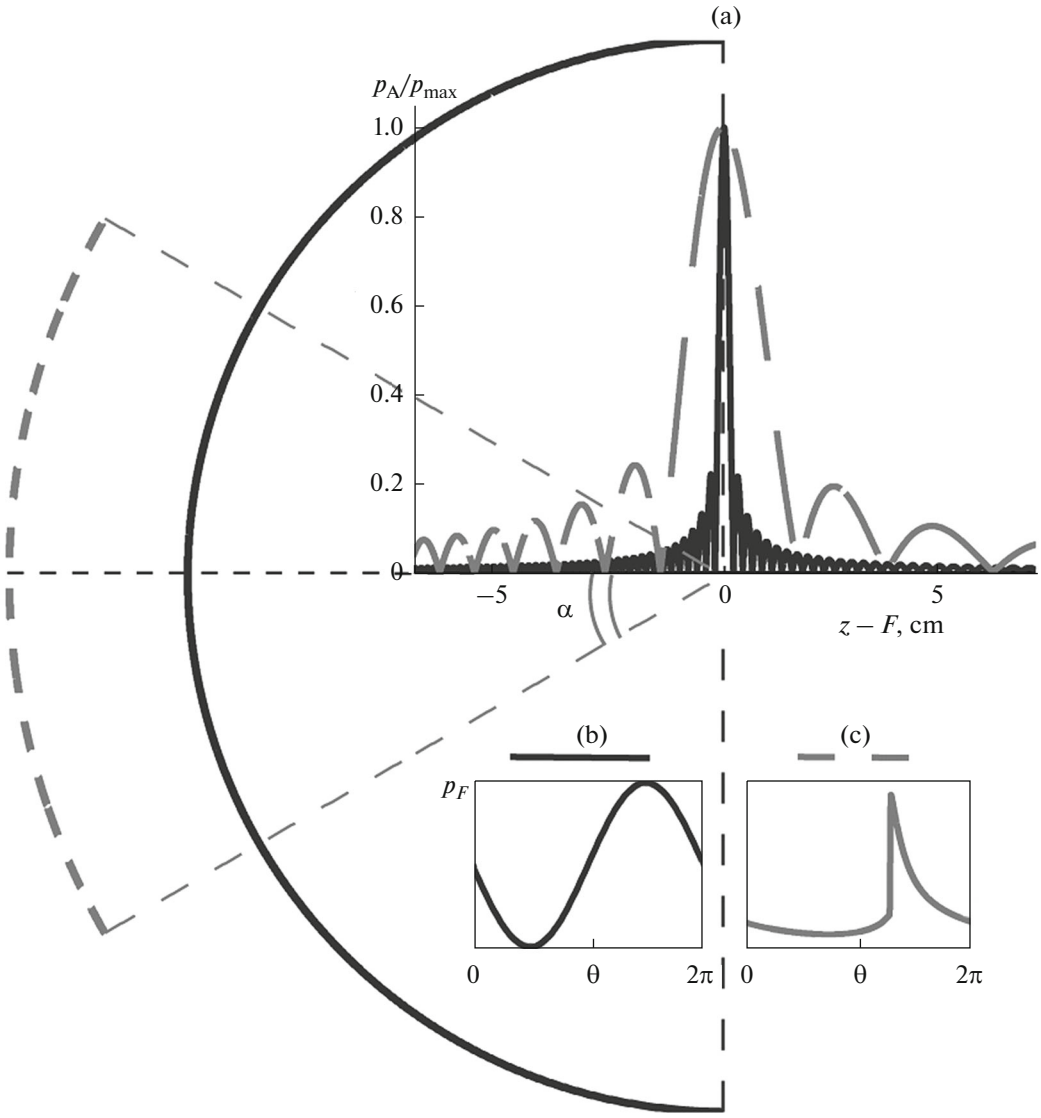

Fig. 1. (a) Pressure amplitude distributions, p_A/p_{max}, along the beam axis normalized to its maximum value for a hemispherical transducer (solid curve, frequency $f = 650$ kHz, focal length $F = D/2 = 15$ cm, and aperture angle $2\alpha = 180°$, where D is the transducer aperture) and a transducer in a shape of a spherical segment (dotted curve, $f = 650$ kHz, $F = D = 20$ cm, and aperture angle $2\alpha = 60°$). (b) Linear pressure waveform at the focus, $p_F(\theta)$, characteristic for generating thermal damage of tissue using a hemispherical transducer. (c) Nonlinear pressure waveform with developed shock at the focus, $p_F(\theta)$, characteristic for mechanical destruction of tissue using a transducer in a form of a spherical segment.

This study evaluates a possibility of designing array transducers in the shape of a spherical segment with an aperture angle of about 60° capable of generating shock fronts at the focus with amplitudes of 80–115 MPa when focusing through the intact skull. Theoretical modeling is employed that accounts for the following uncompensated losses of the ultrasound energy of the beam: frequency-dependent absorption in the skull, reflections at its inner and outer surfaces, and absorption in the brain tissue. It is assumed that aberrations that occur due to the difference in the sound speed in the skull and tissue can be compensated using methods that are being rapidly developed [6–8, 20]. The following parameters were varied in the study: ultrasound frequency in the range of 650 kHz–1.2 MHz, aperture angles, array dimensions, and density of filling the array with elements. The latter is especially important because the relatively low filling factor (55–65% of the total transducer area) makes it possible to use quasi-random or spiral [21, 22] arrangements of the elements, thus extending the capabilities of dynamic focusing [23] but simultaneously limiting the maximum achievable array power. The aim of the study is to determine the values of the

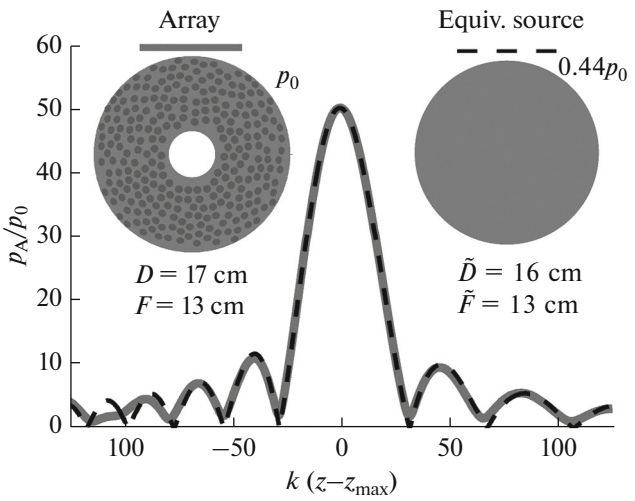

Fig. 2. (a) Distributions of pressure amplitude along the beam axis, p_A/p_0, normalized to the pressure amplitude at the array elements for a 256-element array (solid curve, D is the array aperture diameter, F is focal length, and $\Psi = 0.4$ is a filling factor of the array) and the equivalent spherical transducer (dotted line). Diagrams of the array and equivalent source (front view) and geometric parameters of the array and equivalent source (left and right). Relationships between initial amplitudes at the array elements (p_0) and at the equivalent source ($0.44p_0$) are given.

considered array parameters for which it is possible to achieve shock formation at the focus at a depth of up to 10 cm in the brain tissue given the maximum intensity at the array elements is 40 W/cm^2; the latter is determined by the existing technical limitations [22]. In addition to the advantages of implementing efficient thermal and mechanical tissue ablation and expanding the dynamic focusing region, the proposed arrays will have smaller size and smaller focusing angle of approximately 60° compared to the hemispherical ExAblate arrays. This will make it possible to mechanically move the array relatively to a patient's head thereby decreasing and increasing its distance from the skull, as well as rotating the array around the center of the skull to enable nearly perpendicular passage of the rays from all elements of the array through the skull bones.

THEORETICAL MODEL

In general formulation, the posed problem required a solution to the nonlinear inverse problem of determining the parameters of a multi-element array capable of producing a shock front of a certain amplitude at the focus after ultrasound transmission through the skull bones and brain tissues. This formulation implies multi-parametric simulations of the 3D Westervelt equation taking into account the aberrations and attenuation of the ultrasonic beam on its path to the focus [12, 17]. It is obvious that this approach is very computationally intensive, and the analysis of the results is additionally complicated by a large number of the geometric parameters of the array such as, for example, the coordinates, shape, and size of its elements. Therefore, to solve the formulated problem numerically, a number of simplifying assumptions were used. First, it was assumed that distortions in the field structure related to the skull inhomogeneities are compensated, thus, in this study their influence was neglected. Moreover, an "equivalent" source that is simpler than an array was considered as a boundary condition to the model, and nonlinear acoustic field was simulated using the Khokhlov–Zabolotskaya (KZ) parabolic equation. It was also assumed that the degree of the waveform distortion at the array focus is determined mainly by nonlinear effects in the focal region of the beam [19, 26]. These simplifying assumptions are described below in more detail.

In our previous studies it was shown that each array with quasi axially symmetric geometry can be substituted by a simpler "equivalent source", whose field closely approximates the array field near the focus [26]. Consider an example of a linear field generated in water by an array with operating frequency of 1 MHz, focal length $F = 13$ cm, and diameter $D = 17$ cm, consisting of $N = 256$ circular piston elements with a radius $a = 0.35$ cm (Fig. 2) [24]. We choose a spherical equivalent source with the same operating frequency and focal length $\tilde{F} = F$, while the aperture $\tilde{D}$ and the initial amplitude $\tilde{p}_0$ at the equivalent source will be varied to achieve the best matching of the pressure amplitudes p_A/p_0 on the axis of the array (Fig. 2, solid curve) and the equivalent source (Fig. 2, dotted curve). The best fit parameters are determined by minimizing the functional $\Delta(\tilde{D}, \tilde{p}_0)$ of the discrepancy between the linear array field $p_A(z_i)$ and the equivalent source field $\tilde{p}_A(z_i)$, each of which is a solution to the linearized Westervelt equation within a certain interval on the beam axis:

$$\Delta(\tilde{D}, \tilde{p}_0) = \sum_{z_i \in [A,B]} \left(p_A(z_i) - \tilde{p}_A(z_i)\right)^2. \qquad (1)$$

Here, A and B are the boundaries of the interval on the axis where the distributions $p_A(z_i)$ and $\tilde{p}_A(z_i)$, are compared, and z_i are certain points on the array axis. In the case of multi-element arrays, it is convenient to choose the location of the boundaries A and B at the half-height of the main focal lobe. The array field can be calculated using the approximate analytical solution in the far field of each array element or a

direct numerical calculation of the Rayleigh integral over the array surface [23]. With numerical minimization of the functional (1), the resulting parameters of the spherical equivalent source were found as follows: $\tilde{D} = 16$ cm and $\tilde{p}_0 = 0.44 p_0$. It is seen that axial distributions of the pressure amplitude for the equivalent source and array almost coincide within the interval $[A, B]$. In this case, the geometric parameters of the equivalent source and array transducer are close to each other: $\tilde{F} = F = 13$cm, and the difference between the aperture diameters $|\tilde{D} - D|$ is only 6%. In addition, the ratio between the initial pressure amplitudes at the array elements and the equivalent source surface, $\tilde{p}_0/p_0 = 0.44$, is close to the value of the filling factor of the array, $\Psi = 0.4$. Here, $\Psi = S_{\text{rad}}/S_{\text{tot}}$, $S_{\text{rad}} = N\pi a^2$ is the total area of all array elements and S_{tot} is the total area of the array surface. Indeed, the total areas of the array and equivalent source are close to each other, but only 40% ($\Psi = 0.4$) of the array surface is filled with radiating elements with the pressure amplitude p_0, at each element, as compared with radiation from the entire equivalent source surface with the pressure amplitude $\tilde{p}_0$. It is obvious that for matching the pressures of the linear array field and equivalent source near the focus, it is necessary that the radiating spherical source has the initial amplitude

$$\tilde{p}_0 \approx \Psi p_0. \qquad (2)$$

Thus, an arbitrary array with focal length F, aperture D, filling factor Ψ, and pressure amplitude p_0, at its elements is replaced here in the zero-order approximation by a spherical transducer with the same geometric parameters $\tilde{F} = F$ and $\tilde{D} = D$, and the amplitude $\tilde{p}_0 = \Psi p_0$ at its surface. These approximations reduce the number of parameters that characterize the field of a multi-element array and significantly simplify the solution to the nonlinear inverse problem of determining the parameters of a spherically focused transducer, that generates a shock of a certain amplitude at the focus. Nevertheless, even with such a simplified setting of the boundary condition, the solution to this problem still requires multiple solutions to the Westervelt equation, which is rather difficult to realize for shock-wave focusing conditions.

The next simplification of the theoretical model is associated with the replacement of a spherical transducer and the description of the acoustic field using the Westervelt equation by a flat transducer with a parabolic phase distribution along the transverse coordinate, and the field description using the Khokhlov–Zabolotskaya (KZ) parabolic equation. Analytic solutions obtained in [25] interrelate the diameter, focal distance, and initial pressure amplitude of such spherical and flat transducers. It was also shown that the fields generated by these transducers and governed by the corresponding linearized equations almost completely coincide in both the region of the main diffraction lobe and in several secondary diffraction lobes in front of and behind the focus. Similarly to the first simplifying assumption, in this case, the nonlinear fields in the focal region of the beam, governed by the corresponding nonlinear equations, will also be close to each other [26].

With the two simplifying assumption described above, the problem of multi-parametric modeling of the 3D Westervelt equation for the array is reduced to multi-parametric modeling of the axially symmetric KZ equation, i.e., to a much simpler problem for numerical simulation that has been already studied in detail [19, 27]. When focusing in water is considered, the KZ equation contains only two independent parameters, thus allowing the nonlinear inverse problem to be solved by performing direct numerical simulations in a wide range of these parameters and correlating the field parameters at the focus with the transducer parameters. The authors of [19] obtained this solution to the KZ equation with a boundary condition specified on a plane in the shape of a circular disk and a parabolic phase distribution along the radial coordinate, that provides focusing. The results were generalized in [26] for the case of a single spherically shaped circular transducer and full diffraction Westervelt model.

Consider now in more detail specific nonlinear field properties at the focus of a spherical transducer using the results of the previous studies [19, 26]. For any chosen transducer, with increase of its power, the wave profile at the focus is getting distorted toward forming a shock front, then the shock amplitude increases and gradually reaches a saturation level. The concept of a developed shock at the focus was introduced in [19]. Following the definition of [19], the developed shock corresponds to the condition when its amplitude A_s reaches a maximum relative to the initial pressure p_0 at the transducer surface ($A_s/p_0 = \max$). It was shown that a developed shock can be determined visually in the physical or numerical experiment by the coincidence of its lower boundary with zero pressure level (Fig. 3a). It was also established that the amplitude of the developed shock at the focus is mainly determined by the transducer aperture angle (or its F-number) and is almost completely independent on the transducer aperture. This is illustrated in Fig. 3a for two sources in the shape of a spherical segment with the same F-number ($F_\# = 1$) but different dimensions: the same amplitude of the developed shock is observed at the focus, $A_s \approx 80$ MPa. The

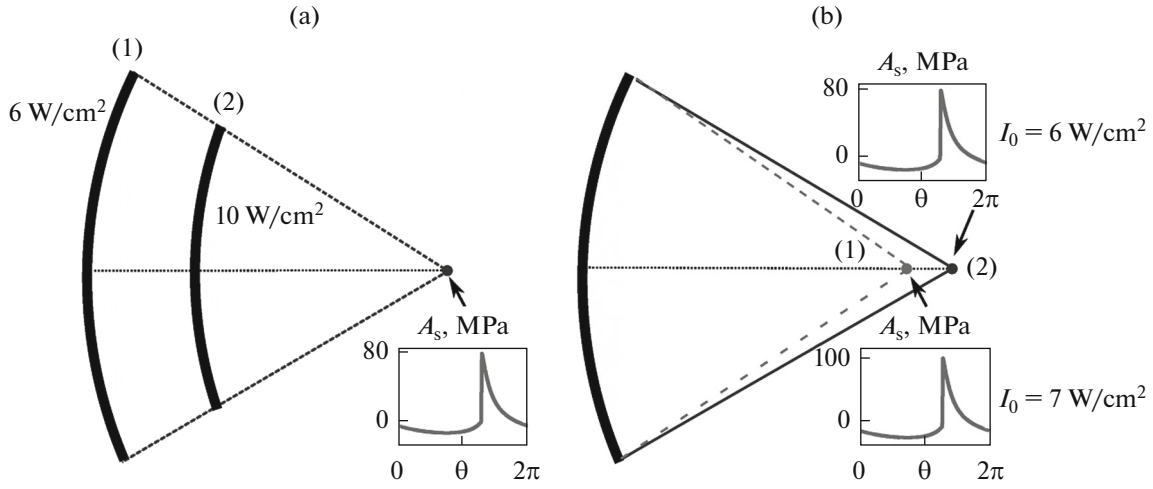

Fig. 3. (a) Wave profile, $p_F(\theta)$, with developed shock at the focus for two transducers with the same $F_\# = 1$ and different apertures (1): $D = 10$ cm, (2): $D = 8$ cm. Initial intensity required to form a developed shock at the focus is indicated near transducer surfaces. (b) Wave profiles, $p_F(\theta)$, with developed shock at the focus for two transducers with different F-numbers: dotted curve (1), $F_\# = 0.9$; solid curve (2), $F_\# = 1$. Initial intensities required to form a developed shock at the focus are given.

amplitudes of the developed shock at the focus are different for transducers with different F-numbers: $A_s \approx 80$ MPa for $F_\# = 1$ and $A_s \approx 100$ MPa for $F_\# = 0.9$. The initial intensity I_0 at the transducer surface required for forming a developed shock at the focus depends on two parameters: the F-number, $F_\#$, and dimensionless transducer aperture kD, where k is the wavenumber. In fact, the initial intensity shown in Fig. 3 is different both for different apertures and identical F-numbers (Fig. 3a) and for different F-numbers and identical apertures (Fig. 3b).

Application of the models described above makes it possible to calculate the developed shock amplitude A_s at the focus and the initial intensity I_0 at the surface of a spherical transducer that provide this amplitude. Further calculation of the nonlinear field at the focus now requires only consideration of ultrasound transmission losses in the skull and brain tissues. Three factors determine the decrease in the pressure level at the focus due to ultrasound propagation through the skull bones: beam defocusing due to aberrations, absorption of an ultrasound wave when passing through the skull, and reflection from its boundaries. The existing time-reversal and phase-conjugation methods make it possible to compensate for aberrations and appreciably reduce the influence of the first type of losses by varying the signal amplitudes and phases at the array elements [8]. Under the assumption that aberrations that occur when ultrasound propagates through skull bones are corrected, the remaining losses due to absorption and reflections are approximated using the dependence $\alpha_n = 5 + 7f$ dB, based on data from measurements with an InSightec array, which were confirmed by independent measurements of other authors in the considered frequency range (0.65–1 MHz); here f is the frequency measured in megahertz [28]. This corresponds to the uncompensated power losses due to transmission through the skull by a factor of

$$S(f) = 10^{(0.5+0.7f)}. \quad (3)$$

To take into account the absorption in brain tissue, an additional compensating factor of 2.1 dB for the initial intensity was introduced, which accounts for absorption at the frequency of 1 MHz at the depth of 10 cm in the brain [29].

As discussed earlier, the main geometric parameter that influences the value of the developed shock amplitude at the focus is the transducer F-number, $F_\#$ [19]. Taking into account that pressure waveforms with shock amplitudes of about 80 MPa are currently successfully used in various tissues with the boiling-histotripsy method [15–17], when the array parameters are chosen, it is most reasonable to choose the F-number close to $F_\# = 1$ (Fig. 3a). For this chosen transducer F-number, the initial intensity I_0, necessary for obtaining a developed shock at the focus depends on the wave size kD of the transducer. When the transducer frequency or its geometric dimensions increase (i.e., with an increase in the parameter kD), the intensity at an element required for forming a developed shock decreases.

The total radiating array area or its filling factor Ψ is another important parameter. At present, randomized arrays with circular elements and with relatively

low filling factor of at most 55–65% are actively used in clinical and research HIFU systems [16, 17, 24]. Such arrays have large dynamic-focusing regions. At the same time, denser arrays are currently being developed [1, 21, 30]. Increasing the filling factor and changing the shape of the elements make it possible to increase the array power while keeping its dimensions, but may lead to impaired abilities to move the focus electronically. In this study, we analyze the possibility of implementing the shock-wave focusing conditions for different filling densities in the range of $\Psi = 0.65$–0.9. The cases of $\Psi = 0.65$ ("sparse array") and $\Psi = 0.8$ ("dense array") are considered separately.

For an array with the operating frequency f, focal length F, aperture D, and filling factor Ψ, it is now possible to formulate the final algorithm for determining the initial intensity at its elements, which is required for forming a developed shock at the transducer focus after propagation through an intact skull and brain tissues:

(1) the array is replaced by a spherical single-element transducer of the same frequency f and the same geometric parameters $\tilde{F} = F$ and $\tilde{D} = D$;

(2) for this spherical transducer, the amplitude of the developed shock A_s at the focus and the initial intensity $\tilde{I}_0$, at which the developed shock is formed, are determined using the results of [19, 25, 26];

(3) based on the equation (2) and losses $S(f)$ (3) for ultrasound propagation through the skull bones, the amplitude of the developed shock A_s is reached at the following intensity at the array element: $I_0 = \tilde{I}_0 \Psi^{-2} S^{-1}$.

The initial intensity I_0, was calculated for frequencies $f = 0.65$–1.2 MHz, focal lengths $F = 15$–21 cm, F-numbers $F_\# = F/D = 0.85$–1, and filling factors of the array $\Psi = 0.65$–0.9. Focusing through an intact skull in water was considered, then a correction for losses in brain tissues was introduced, showing that for the formation of a shock in the case of focusing in tissue at initial intensity of 40 W/cm^2, it should be formed at initial intensity of 25 W/cm^2 in the case of focusing in water. Correspondingly, the obtained I_0 values were compared with the maximum of 25 W/cm^2; on this basis, it was concluded that it is possible to implement the shock-wave forming conditions for the given parameters at a given depth.

RESULTS

Figure 4 shows the dependences of the initial intensity I_0 at the elements of a "dense" array ($\Psi = 0.8$), required for formation of developed shocks at the focus when focusing through the skull in water, on the focal length F for the $F_\# = 1$ and frequencies $f = 0.8$, 1, and 1.2 MHz. Horizontal dashed lines show the levels of the maximum possible intensity: 40 W/cm^2 if the absorption in the brain tissue can be neglected, and 25 W/cm^2 if the absorption corresponding to a depth of 10 cm and a frequency of 1 MHz is compensated. It is seen that for the dense arrays, formation of the developed shocks at all depths ($I_0 < 25$ W/cm^2) at $f = 0.8$ MHz is possible if the array diameter exceeds 22.5 cm, while at frequencies of 1 and 1.2 MHz, the apertures of 20 and 19 cm, respectively, are sufficient.

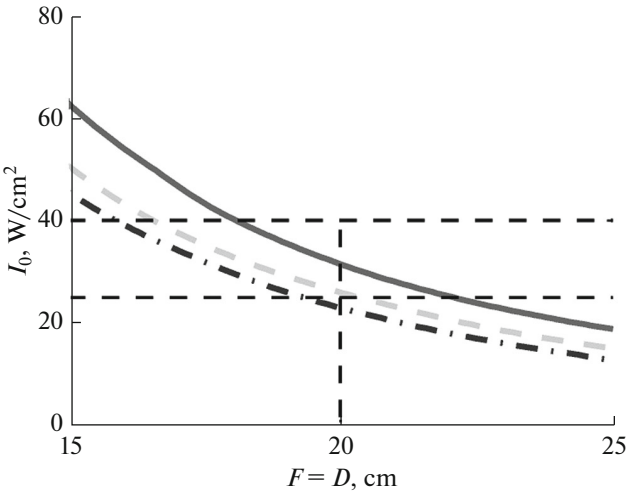

Fig. 4. Dependence of the initial intensity I_0 at the array element required to form developed shocks at the focus when focusing through a skull on focal length F: (solid curve) frequency $f = 800$ kHz, (dotted curve) $f = 1$ MHz, and (dashed–dotted curve) $f = 1.2$ MHz. Horizontal lines indicate technically achievable intensity maxima at the array elements with (25 W/cm^2) and without (40 W/cm^2) accounting for losses in brain tissues. Arrays with F-number $F_\# = 1$ and filling factor $\Psi = 0.8$ are considered.

Consider now an array with a focal length $F = 20$ cm and $F_\# = 0.9$ and 1. We investigate the dependence of the initial intensity I_0 at the array element required to form a developed shock at the focus after propagation through the skull on the operating frequency f in the range $0.65\ \text{MHz} \le f \le 1.1\ \text{MHz}$. Figure 5a shows that for compact arrays with $F_\# = 1$ (bold solid curve), implementation of the developed shock focusing conditions is possible for frequencies higher than 1 MHz and for strongly focused arrays with $F_\# = 0.85$ (bold dashed curve) – for frequencies higher than 0.85 MHz. For a "sparse array" (thick curves) implementation of shock-forming focusing without excessing the threshold intensity level at the array surface is nearly impossible. Thus, increasing the density of filling the array with its elements is an important factor that can reduce the initial intensity required to form developed shocks

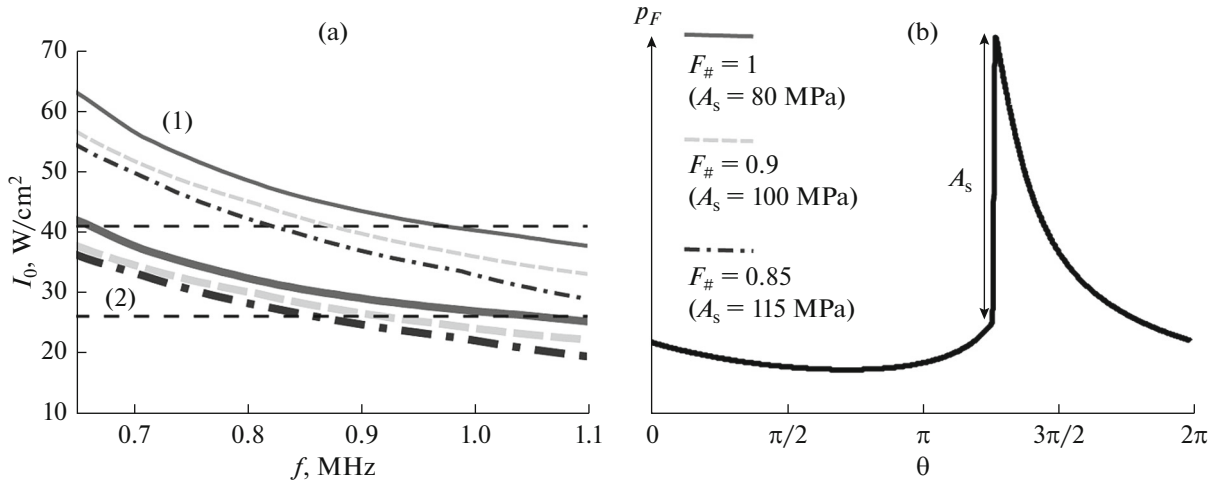

Fig. 5. Dependence of (a) initial intensity I_0 at the array elements required to form developed shocks at the focus when focusing through a skull on frequency f: (thin curve) (1) sparse array with the filling factor $\Psi = 0.65$, (bold curves); (2) dense array with $\Psi = 0.8$. For solid curves, $F_\# = F/D = 1$; for dotted curves, $F_\# = 0.9$; and for dashed–dotted curves, $F_\# = 0.85$. Horizontal lines indicate technically achievable intensity maxima at the array elements with (25 W/cm^2) and without (40 W/cm^2) accounting for losses in brain tissues. Arrays with focal length $F = 20$ cm are considered. (b) Wave profile at focus $p_F(\theta)$ with developed shock of amplitude A_s. Values of shock amplitudes A_s for cases considered in curve (a) are given in Fig. 5b.

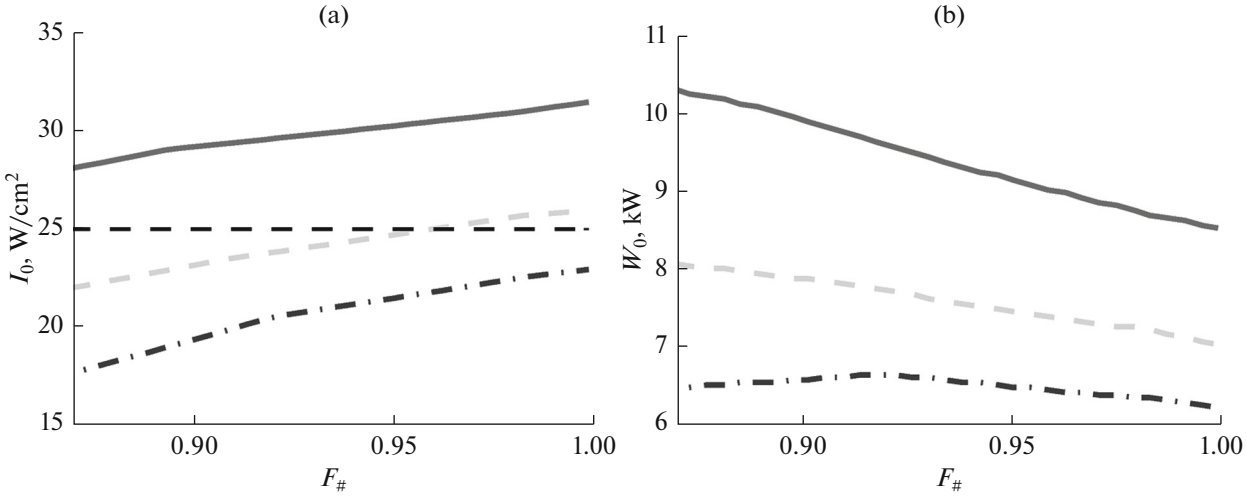

Fig. 6. Dependences of (a) initial intensity I_0 at the array elements and (b) the total array power W_0 required to form developed shocks at the focus when focusing through a skull on array F-number $F_\#$: (solid curve) frequency $f = 800$ kHz, (dotted curve) $f = 1$ MHz, and (dashed–dotted curve) $f = 1.2$ MHz. Horizontal line indicates the technically achievable intensity maximum at the array elements with account for losses in brain tissues: 25 W/cm^2. Arrays with focal length $F = 20$ cm and filling factor $\Psi = 0.8$ are considered.

at the focus. In addition, more focused transducers, i.e., those with larger aperture and the same focal length, are preferable. Figure 5a shows these cases of smaller $F_\#$ (dotted ($F_\# = 0.9$) and dashed–dotted ($F_\# = 0.85$) curves) for both the dense and sparse arrays. However, it should be taken into account that a decrease in the value of $F_\#$ leads to an increase in the shock amplitude at the focus (Fig. 5b). For example, for $F_\# = 0.9$, the amplitude of the developed shock increases to $A_s = 100$ MPa, while for $F_\# = 0.85$, it reaches $A_s = 115$ MPa. In the latter case, the intensity I_0 can be decreased to 20 W/cm^2 (bold dashed–dotted line) for the frequency of 1.1 MHz. The effect of the F-

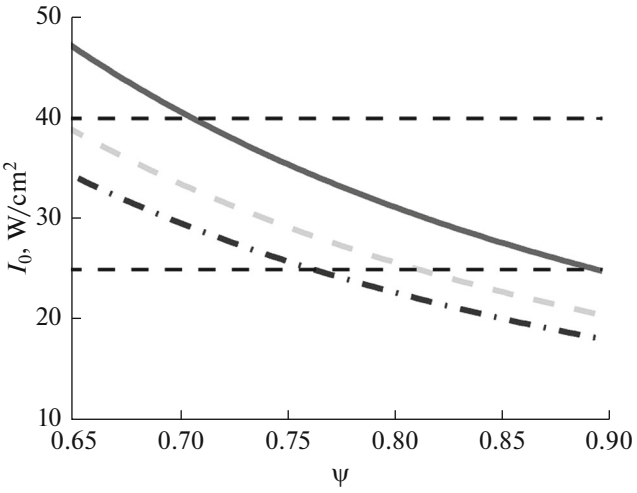

Fig. 7. (a) Dependence of the initial intensity I_0 at the array elements required to form developed shocks at focus when focusing through a skull on the filling factor Ψ of the array: (solid curve) frequency $f = 800$ kHz, (dotted curve) $f = 1$ MHz, and (dashed–dotted curve) $f = 1.2$ MHz. Horizontal lines indicate technically achievable intensity maxima at the array elements with (25 W/cm^2) and without (40 W/cm^2) accounting for losses in brain tissues. Arrays with focal length $F = 20$ cm and F-number $F_\# = 1$ are considered.

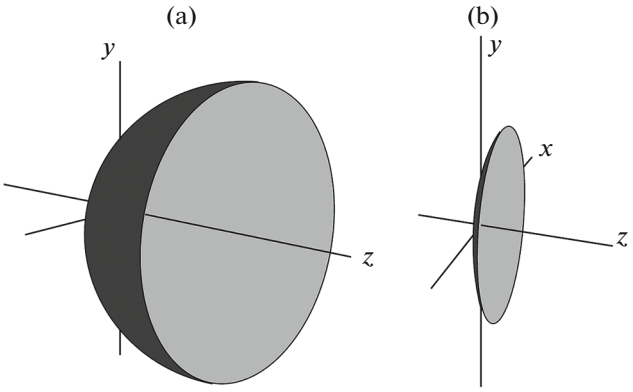

Fig. 8. (a) Hemispherical array similar to ExAblate-type systems ($F = D/2 = 15$ cm). Here, F is the focal length and D is transducer aperture. (b) Array in the form of a spherical segment with the aperture angle of 60° proposed in this study ($F = D = 20$ cm, the operating frequency 1 MHz, and filling factor Ψ = 0.8).

number is shown in more detail in Fig. 6, where the dependences of the initial intensity I_0 (Fig. 6a) and total power W_0 (Fig. 6b) of the array required to form a developed shock at the focus on its F-number are shown for three different frequencies of the array with a fixed focal length of 20 cm.

Consider now the influence of the filling factor of the array Ψ on the initial intensity I_0 at the elements of the array with $F = 20$ cm and $F_\# = 1$ (Fig. 7). Transducers with such an aperture angle are used most frequently for boiling-histotripsy applications [13, 15–17]. Increasing the filling factor of the array makes it possible to considerably reduce the initial intensity I_0: for the case of low frequencies ($f = 0.8$ MHz), to values lower than 25 W/cm^2 for very high filling factors (Ψ > 0.9, bold solid curve); for $f = 1$ MHz, beginning with Ψ > 0.82 (dashed curve); and for $f = 1.2$ MHz, beginning with Ψ > 0.77 (dashed–dotted curve). Despite the low initial intensity levels I_0 obtained for arrays highly populated with elements (Ψ = 0.9), additional evaluation of their dynamic focusing capabilities are needed, while for arrays with lower densities of element population (Ψ = 0.6–0.65), strong capabilities of electronic focus steering have been demonstrated [22].

CONCLUSIONS

We have evaluated the possibility of using multi-element focusing transducers for surgical destruction of deep brain tissues through an intact skull using nonlinear pulsed–periodic irradiation protocols that provide shock-wave-mediated effects at the focus. In contrast to thermal damage of brain structures in the continuous irradiation mode of relatively low focal pressures used in ExAblate-type systems, irradiation with high-power ms-long tone-bursts with shock fronts would enable mechanical tissue ablation (boiling histotripsy) in the focal region of the beam without appreciable heating of tissues surrounding the targeted region and without overheating the skull bones [15].

For transcranial boiling histotripsy, a model of an array in the form of a spherical segment with an aperture angle of 60° was proposed ($F = D = 20$ cm, $F_\# = 1$; its aperture is 33% smaller and the aperture angle is three times smaller than those in a 30-cm-diameter hemispherical array of the ExAblate system (Fig. 8). As compared to ExAblate-type arrays (Fig. 8a), due to the small aperture angle, the proposed compact array (Fig. 8b) makes it possible to increase the region of dynamic-focusing and to move mechanically the array toward or away from the skull, and also to rotate it relatively to the patient's head. The amplitude of the developed shock front at the focus of the proposed transducer is approximately 80 MPa, which corresponds to successfully realized boiling histotripsy treatments of various tissues, including brain [16]. The conditions for formation of the developed shock fronts at the focus required for boiling histotripsy were estimated taking into account frequency-dependent losses due to reflection and absorption in the skull and

in brain tissue assuming that aberrations are completely compensated. Simulations showed that shock formation conditions, given the initial intensity at the array elements does not exceed a characteristic technological maximum (40 W/cm^2), is possible only for a sufficiently tightly packed array. Note that the results of this study are given for the case of ultrasound focusing in water; focusing to different depths in tissue requires an additional increase in intensity that compensates the losses in tissue, which is, e.g., 0.21 dB/cm/MHz$^{1.18}$ [1, 29]. For example, at a maximum depth of 10 cm and a frequency of 1 MHz, the intensity must be increased by 60%; thus, the conditions of developed shocks in case of focusing in water should be achieved at the intensity of 25 W/cm^2. Simulations also showed that for a compact array with the proposed geometry (Fig. 8b) and filling factor of $\Psi = 0.8$, shock-forming conditions in brain tissues can be technically implemented starting from 1.05 MHz, while for currently existing sparse arrays with quasi-random element arrangement ensuring large electronic steering capabilities, the shock-forming conditions cannot be achieved up to 1.2 MHz.

Possibilities of additional reduction in the initial intensity at the array elements were revealed: It is shown that the reduction can be achieved by the increase of frequency and the filling factor of the array, and also by augmenting the array aperture with preservation of either its F-number or focal length. Here, strong increase of absorption should be noted at frequencies exceeding 1.5 MHz, because the ultrasound wavelength becomes comparable to the dimensions of inhomogeneities in the inner structure of the skull bones. Currently, new arrays with quasi-randomly arranged elements and a filling factor of almost 100% are under development. This may be the main approach for reducing the initial intensity at the array surface [30]. The use of large arrays is limited by technical features of MRI systems. Increasing the aperture angle of a transducer (or reducing the $F_\#$ parameter) also allows the reduction of the initial intensity, but in this case, the increase in the developed shock amplitude at the focus should be taken into account.

Lastly, taking these factors into account, we have proposed an array model with $F = D = 20$ cm, an operating frequency of 1 MHz, and a filling factor of $\Psi = 0.8$, which is capable of realizing shock-forming conditions at the focus in water through the skull bones for intensities of less than 25 W/cm^2 at the array elements (Fig. 8b). This gives a substantial reserve for compensating additional absorption losses in brain tissues [1, 29]. It should be also noted that the results yield the estimated dependences of the developed shock amplitude at the focus and the initial intensity required at the array elements for these shock-forming conditions. For an array with a particular arrangement and shape of radiating elements, additional refinement of the results is required based on more precise equivalent source simulations (Fig. 2).

In conclusion, this study has shown theoretical feasibility of implementing shock-wave irradiations of deep brain structures through intact skull using multi-element compact phased arrays with an increased filling factor.

ACKNOWLEDGMENTS

This study was supported by the Russian Foundation for Basic Research (project nos. 15-02-00523 and 16-02-00653) and the Council for Grants of the President of the Russian Federation in Support of Leading Scientific Schools (NSh-7062.2016.2).

REFERENCES

1. L. R. Gavrilov, *Focused Ultrasound of High Intesity in Medicine* (Fazis, Moscow, 2013) [in Russian].
2. W. J. Elias, D. Huss, T. Voss, J. Loomba, M. Khaled, E. Zadicario, R. C. Frysinger, S. A. Sperling, S. Wylie, S. J. Monteith, J. Druzgalm, B. B. Shahm, M. Harrison, and M. Wintermark, The New England J. Med. **369** (7), 640–648 (2013).
3. N. McDannold, G. Clement, P. Black, F. Jolesz, and K. Hynynen, Neurosurgery **66** (2), 323–332 (2010).
4. S. Monteith, R. Medel, N. F . Kassell, W. Wintermark, M. Eames, J. Snell, E. Zadicario, J. Grinfeld, J. P. Sheehan, and W. J. Elias, J. Neurosurgery **118** (2), 319–328 (2013).
5. D. Jeanmonod, B. Werner, A. Morel, L. Michels, E. Zadicario, G. Schiff, and E. Martin, Neurosurg. Focus. **32** (1), E1 (2012).
6. J. L. Thomas and M. A. Fink, IEEE Trans. Ultrason. Ferroelectr. Freq. Control. **43** (6), 1122–1129 (1996).
7. K. Hynynen and F. A. Jolesz, Ultrasound Med. Biol. **24** (2), 275–283 (1998).
8. K. Hynynen and R. M. Jones, Phys. Med. Biol. **61** (1), 206–248 (2016).
9. O. A. Sapozhnikov, P. B. Rosnitskiy, and V. A. Khokhlova, in *Program of 5th FUSF*, 2016.
10. H. Odéen, J. de Bever, S. Almquist, A. Farrer, N. Todd, A. Payne, J. W. Snell, D. A. Christensen, and D. L. Parker, J. Therapeutic Ultrasound **2**, Art. 19 (2014).
11. P. B. Rosnitskiy, S.A. Il'in, O. A. Sapozhnikov, and V. A. Khokhlova, Uchen. Zapiski Fiz. Fak. Mos. Univ. **4**, 134301 (2013).
12. P. V. Yuldashev, S. M. Shmeleva, S. A. Ilyin, O. A. Sapozhnikov, L. R. Gavrilov, and V. A. Khokhlova, Phys. Med. Biol. **58** (8), 2537–2559 (2013).
13. V. A. Khokhlova, J. B. Fowlkes, Y. N. Wang, and C. A. Cain, Int. J. Hyperthermia **31** (2), 145–162 (2015).
14. J. Parsons, C. Cain, G. Abrams, and J. Fowlkes, Ultrasound Med. Biol. **32** (1), 115–129 (2006).

15. T. D. Khokhlova, M. S. Canney, V. A. Khokhlova, O. A. Sapozhnikov, L. A. Crum, and M. R. Bailey, J. Acoust. Soc. Am. **130** (5), 3498–3510 (2011).

16. T. Looi, V. A. Khokhlova, C. Mougenot, K. Hynynen, and J. Drake, in *Program Booklet of the 16th Int. Symp. Therapeutic Ultrasound* (Tel Aviv, Israel, 2016) pp. 64–66.

17. W. Kreider, P. V. Yuldashev, O. A. Sapozhnikov, N. Farr, A. Partanen, M. R. Bailey, and V. A. Khokhlova, IEEE Trans. Ultrason., Ferroelect., Freq. Contr. **60** (8), 1683–1698 (2013).

18. H. T. O'Neil, J. Acoust. Soc. Am. **21** (5), 516–526 (1949).

19. P. B. Rosnitskiy, P. V. Yuldashev, and V. A. Khokhlova, Acoust. Phys. **61** (3), 301-307 (2015).

20. S. A. Tsysar, V. A. Khokhlova, V. D. Svet, A. M. Molotilov, W. Kreider, and O. A. Sapozhnikov, in *IEEE Int. Ultrasonics Symp. Proc*. (Tours, France, 2016).

21. L. R. Gavrilov, O. A. Sapozhnikov, and V. A. Khokhlova, Bull. Russ. Acad. Sci.: Phys. **79** (10), 1232–1237 (2015).

22. V. A. Khokhlova, P. V. Yuldashev, P. B. Rosnitskiy, A. D. Maxwell, W. Kreider, M. R. Bailey, and O. A. Sapozhnikov, in *Proc. 45th Ann. Symp. Ultrasonic Industry Assoc.* (Seattle, USA, 2016),

23. S. A. Ilyin, P. V. Yuldashev, V. A. Khokhlova, P. B. Rosnitskiy, O. A. Sapozhnikov, and L. R. Gavrilov, Acoust. Phys. **61** (1), 52-59 (2015).

24. J. W. Hand, A. Shaw, N. Sadhoo, S. Rajagopal, R. J. Dickinson, and L. R. Gavrilov, Phys. Med. Biol. **54** (19), 5675–5694 (2009).

25. P. B. Rosnitskiy, P. V. Yuldashev, V. A. Khokhlova, and B. A. Vysokanov, Acoust. Phys. **62** (2), 151–159 (2016).

26. P. B. Rosnitskiy, P. V. Yuldashev, O. A. Sapozhnikov, A. D. Maxwell, W. Kreider, M. R. Bailey, and V. A. Khokhlova, IEEE Trans. Ultrason., Ferroelect., Freq. Contr. 2017 (accepted).

27. O. V. Bessonova, V. A. Khokhlova, M. R. Bailey, M. S. Canney, and L. A. Crum, Acoust. Phys. **55** (4–5), 463-473 (2009).

28. L. Marsac, Focalisation ultrasonore adaptative et application à la thérapie du cerveau // Paris 7. Ph. D. thesis. 2013.

29. S. A. Goss, L. A. Frizzell, and F. Dunn, Ultrasound Med. Biol. **5** (2), 181–186 (1979).

30. P. Ramaekers, M. Ries, C. T. Moonen, and M. de Greef, in *Program of the 15th Int. Symp. for Therapeutic Ultrasound* (2015) p. 174.

Translated by A. Seferov